General method to evaluate substrate surface modification techniques for light extraction enhancement of organic light emitting diodes

B. C. Krummacher,[a] M. K. Mathai, V. Choong, S. A. Choulis, and F. So
OSRAM-Opto Semiconductors, Inc., 3870 N 1st Street, San Jose, California 95134

A. Winnacker
Department of Material Science VI, University of Erlangen–Nuremberg, Martensstrasse 7, 91058 Erlangen, Germany

(Received 30 September 2005; accepted 19 June 2006; published online 1 September 2006)

The external light output of organic light emitting diodes (OLEDs) can be increased by modifying the light emitting surface. The apparent light extraction enhancement is given by the ratio between the efficiency of the unmodified device and the efficiency of the modified device. This apparent light extraction enhancement is dependent on the OLED architecture itself and is not the correct value to judge the effectiveness of a technique to enhance light outcoupling due to substrate surface modification. We propose a general method to evaluate substrate surface modification techniques for light extraction enhancement of OLEDs independent from the device architecture. This method is experimentally demonstrated using green electrophosphorescent OLEDs with different device architectures. The substrate surface of these OLEDs was modified by applying a prismatic film to increase light outcoupling from the device stack. It was demonstrated that the conventionally measured apparent light extraction enhancement by means of the prismatic film does not reflect the actual performance of the light outcoupling technique. Rather, by comparing the light extracted out of the prismatic film to that generated in the OLED layers and coupled into the substrate (before the substrate/air interface), a more accurate evaluation of light outcoupling enhancement can be achieved. Furthermore we show that substrate surface modification can change the output spectrum of a broad band emitting OLED. © *2006 American Institute of Physics*. [DOI: 10.1063/1.2234550]

I. INTRODUCTION

In the recent years the activities to develop solid state lighting based on organic electroluminescent devices are on the rise. The possibility of producing a flat large area lighting panel in a cheap and simple process will drive creative products and open exciting fields of application. However, one evident drawback is still the low light out-coupling efficiency of organic light emitting diodes (OLEDs). The mismatch of the refractive index between air and the OLED leads to most of the generated light being lost through total internal reflection (TIR) into wave guiding modes and self-absorption. As indicated in Fig. 1, the light emitted by the device can be classified into three modes: the external mode, the substrate waveguided mode, and the anode/organic waveguided mode. Depending on the value of the emission angle with respect to the normal to the susbrate, the generated photons are outcoupled or waveguided into the substrate and the active layers, respectively.

Many approaches have been utilized to increase the outcoupling efficiency. These can be divided into six generic schemes. (1) The patterning of polymer microlens array on the substrate surface,[1] or placing a large size index matching hemispherical lens on top of the substrate.[2] (2) Introducing scattering effects at the substrate surface by means of techniques such as applying a transparent coating on the substrate with embedded small particles,[3] or texturing the substrate surface (for example, by sand blasting[4] or sand paper[5]). (3) Incorporating the light emitting diode in a reflecting mesa structure.[6] (4) Inserting an extremely low refractive index ($n \approx 1.03$) silica aerogel porous layer between the indium tin oxide (ITO) transparent anode and the glass substrate.[7] (5) Increasing light outcoupling efficiency by means of microcavity effects due to the double mirror structure of the organic light emitting device given by both electrodes and the organic layers embedded in between.[8,9] (6) Application of lateral periodic nanostructures on the substrate leading to increase of light outcoupling through Bragg scattering.[10,11]

Using the approaches of schemes (1) and (2), the waveguided light retained within the substrate of the unmodified device (standard flat glass substrate) is extracted. The improvement in light outcoupling by various methods of modifying the substrate surface is often quantified by an ap-

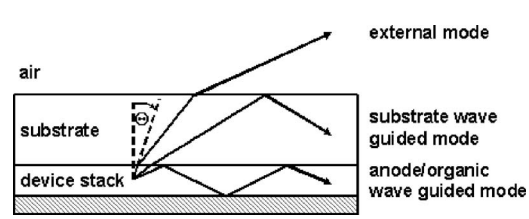

FIG. 1. The external mode the substrate waveguided mode, and the anode/organic waveguided mode in an organic EL device. Dependent on the emission angle Θ the generated photons are out coupled or waveguided.

[a]Electronic mail: benjamin.krummacher@osram-os.com

 © 2006 American Institute of Physics

Pictiva EX2014
Samsung v Pictiva
IPR2024-00855

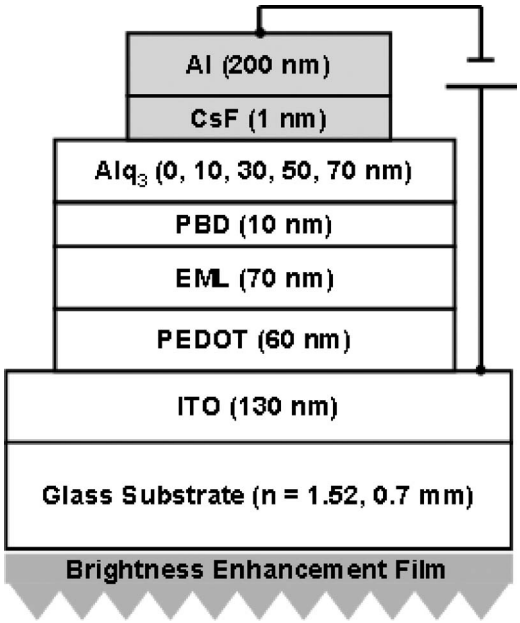

FIG. 2. Structure of the OLEDs used in this study.

parent enhancement factor, $k=\eta_2/\eta_1$, where η_1 is the efficiency of the unmodified OLED and η_2 is the efficiency of the device after modifying the substrate.

In this paper we show a strong dependence of the enhancement factor k on the device architecture itself. Furthermore we demonstrate an alternative method to determine the enhancement of light extraction using light outcoupling approaches of scheme (1) or (2) discussed earlier. The proposed method thus eliminates dependence on device architecture which would otherwise lead to inaccurate conclusions regarding the efficiency of the device itself.

II. EXPERIMENTAL AND SIMULATION DETAILS

A. Fabrication of OLEDs

Figure 2 shows the structure of the green emitting OLEDs (peak wavelength $\lambda=510$ nm) used in this study. Each substrate has four individual OLEDs with a 0.4 cm^2 active area. The glass substrate has a thickness of 0.7 mm and a refractive index $n=1.52$. The OLEDs are fabricated as follows. ITO coated glass substrates were patterned using standard photolithographic techniques. This was followed by cleaning of the ITO surface including wash steps with deionized (DI) water. In addition, the ITO substrates were subjected to oxygen plasma treatment for 10 min. A thin (60 nm) film of poly(3,4)-ethylendioxythiophene doped with poly(styrene sulfonate) (PEDOT:PSS) was spin coated atop the ITO and then baked for 30 min at 200 °C. The green emitting layer (EML) was then spin coated on the top of the PEDOT:PSS with conditions to yield a light emitting layer thickness of around 70 nm. The light emitting layer was then annealed at 80 °C for 30 min. The solution for the EML consisted of 24% (wt) 2-(4-biphenyl)-5-(4-*tert*-butylphenyl)-1,3,4-oxadiazole (PBD), 9% (wt) 4,4′-bis(*m*-tolylphenylamino)biphenyl (TPD), 6% (wt) fac-tris(2-phenylpyridine)iridium $Ir(ppy)_3$, and 61% (wt) polyvinylcarbazole (PVK) in chlorobenzene.[12] On the top of the EML a hole-blocking layer consisting of 2-(4-biphenyllyl)-5-(4-*tert*-butylphenyl)-1,3,4-oxadiazole (PBD) was thermally evaporated in a vacuum coater to a thickness of 10 nm. This was followed by thermal evaporation of a tris(8-hydroxyquinoline) aluminium (Alq_3) layer on top of the PBD layer. Devices with five different Alq_3-layer thicknesses (0, 10, 30, 50, and 70 nm) were prepared. Then a caesium fluoride (CsF) layer with a thickness of 1 nm was deposited as an electron injection layer. Finally an Al layer with a thickness of 200 nm was deposited as the cathode. All the thermally evaporated layers were deposited in a vacuum coater sequentially in a single pump down cycle. Following evaporation of the cathode, the devices were encapsulated with a glass lid and getter. All device fabrication steps from the EML spin coating to device encapsulation were carried out in an inert nitrogen atmosphere.

B. Brightness enhancement film

After measuring the light output of the unmodified devices (the method is described in more detail below), a brightness enhancement film (BEF) prepared from 3M (Vikuiti BEF II 90/50) was applied on the surface of the devices. The BEF film consists of an acrylic resin with prismatic features on its surface coated on a polyester substrate. The prism angle is 90° and the prism pitch is 50 μm. The BEF film has a nominal thickness of 155 μm and was optically coupled to the glass substrate with optical laminating tape (3M No. 8141, $n=1.49$).

C. Measurement of substrate mode and external mode intensities

The OLED emission intensity was measured using a large area (18×18 mm^2) Si photodiode according to a method described by Nakamura *et al.*[13] The distance between the Si photodiode and the OLED substrate's surface was kept at <0.5 mm. Considering the size of the OLED's active area in comparison to the area of the Si photodiode, this setup offers a nearly entire solid angle collection of the light emitted by the devices. Measurements were carried out alternatively with an air gap and an optical gel obtained by Norland whose refractive index was 1.56. When the air gap was filled with gel, TIR at the glass/air interface disappeared, enabling the emitted light of the external and substrate waveguided modes to be measured by the Si photodiode simultaneously. Thus three intensities I_{air}, I_{gel}, and I_{film} were measured, where I_{air} and I_{gel} were the emission intensities detected by the Si photodiode at the air and gel gaps before modifying the device, and where I_{film} was the emission intensity detected at the air gap after applying the BEF film. All intensities were measured at a current density of 1 mA/cm^2.

D. Simulation of microcavity effects

Optical simulation of the experimental results was performed using the microcavity simulation tool UNIMCO 4.0 by UNICAD.[14] The radiative emission from the recombining excitons is modeled by oscillating dipoles in front of a mirror.[15] The recombining exciton is modeled as a two-level system whose transition rate is given by Fermi's golden rule.[16] The

Pictiva EX2014
Samsung v Pictiva
IPR2024-00855

method used in UNIMCO is based on the transfer matrix formalism including additional source terms for electric field (i.e., the dipole emission terms). The electric field emitted by electric dipoles can be expressed in terms of superposition of s-(TE) and p-(TM) polarized waves, while the dipole source can be decomposed into three orthogonal components (d_s, d_p, d_v), where d_s and d_p are in-plane dipole components and d_v is the out-of-plane component. It can be shown that the powers per solid angle θ and surface emitted by such dipoles in an unbounded medium of refractive index n_{emit} are of the form

$$P_0^s = \frac{3}{8\pi}, \tag{1a}$$

$$P_0^p = \frac{3}{8\pi}\cos^2\theta, \tag{1b}$$

$$P_0^v = \frac{3}{8\pi}\sin^2\theta. \tag{1c}$$

For a sheet of dipoles at distance z from the cathode reflector, the power per unit solid angle and surface $P_{\text{front}}^{s,p,v}$ radiated outside the microcavity by the s, p, and v dipoles can be calculated from the following equations:

$$P_{\text{front}}^s = |1 + r_1^s e^{2i\varphi^i}|^2 \frac{1 - |r_2^s|}{|1 - r_1^s r_2^s e^{2i\varphi}|^2} P_0^s, \tag{2a}$$

$$P_{\text{front}}^p = |1 + r_1^p e^{2i\varphi^i}|^2 \frac{1 - |r_2^p|}{|1 - r_1^p r_2^p e^{2i\varphi}|^2} P_0^p, \tag{2b}$$

$$P_{\text{front}}^v = |1 + r_1^v e^{2i\varphi^i}|^2 \frac{1 - |r_2^v|}{|1 - r_1^v r_2^v e^{2i\varphi}|^2} P_0^v, \tag{2c}$$

where r_1 is the reflectivity coefficient of the anode mirror and r_2 the reflectivity of the cathode mirror of the microcavity, φ and φ^I are given by

$$\varphi = \frac{2\pi z}{\lambda} n_{\text{emit}} \cos\theta_{\text{emit}}, \tag{3}$$

$$\varphi^I = \frac{2\pi d}{\lambda} n_{\text{emit}} \cos\theta_{\text{emit}}, \tag{4}$$

where λ is the wavelength of the emitted light and d is the optical path length.

Only the radiation emitted in the source medium (refractive index n_{emit}) with angles θ_{emit} smaller than the critical angle: $\theta_{\text{emit}}^0 = \arcsin(n_a/n_{\text{emit}})$, where n_a is the refractive index of the outside medium, can be extracted out of the microcavity. The interval $[0, \theta_{\text{emit}}^0]$ corresponds to the escape window of the radiation. If $\theta_{\text{emit}} > \theta_{\text{emit}}^0$, the light will undergo total internal reflection. The amount of extracted light is a fraction of the light generated in a distance z from the cathode,

$$P_{\text{extr}}^{s,p,v} = P_{\text{front}}^{s,p,v} \quad \text{for } 0 \leqslant \theta_{\text{emit}} \leqslant \theta_{\text{emit}}^0. \tag{5}$$

Considering an emission zone profile $E(z)$ $(0 < z < Z)$, the total power radiated out of the device is given by

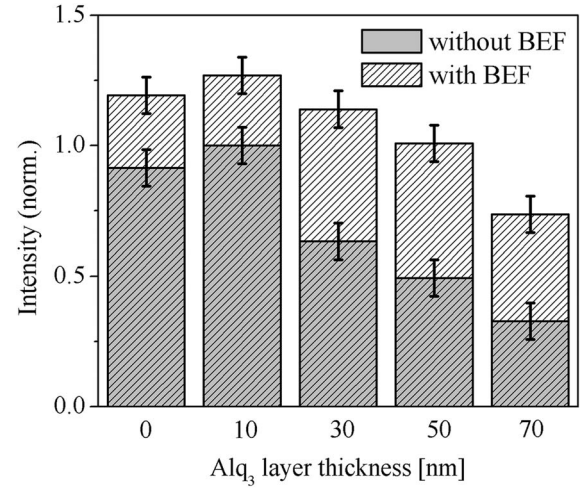

FIG. 3. Light output of the devices before and after applying the brightness enhancement film. The intensities are normalized on the output of the light output of the device with a Alq_3-layer thickness of 10 nm. The error bars represent the standard deviations of the measured values.

$$P_{\text{total}}^{s,p,v} = \int_0^Z E(z)dz \int_0^{\theta_{\text{emit}}^0} \sin\theta d\theta \int_0^\infty d\lambda P_{\text{front}}^{s,p,v}(\theta,\lambda). \tag{6}$$

Further refinements are based on the optical constants as a function of wavelength for all layers of the device stack, which were determined by standard ellipsometry.

Considering Eqs. (1)–(6), it is obvious that the variation in the location exciton profile $[E(z)]$ formed within the LEP can result in significant differences in the extent to which light can be out coupled from the device due to the presence of a microcavity in the OLED stack.

Without substrate surface modification, the light at the radiation angle below θ_1 escapes from the device as an external mode, that between θ_1 and θ_2 gets trapped in the glass as a substrate waveguided mode, and that above θ_2 is coupled into the ITO layer as a result of anode/organic waveguiding (Fig. 1).

III. RESULTS AND DISCUSSION

Figure 3 shows the external light output of the devices before and after applying a BEF film as a function of the Alq_3 thickness. It was independently confirmed that the emission from the device originated from $Ir(mppy)_3$ with negligible (if any) emission from Alq_3. It is observed that with increasing Alq_3 thickness the light output in both cases (i.e., without and with the BEF film) decreases. The intensity I_{air}, which is equal to the light output of the device before applying the BEF film, decreases with increasing values of Alq_3 layer thickness to 1/3 of the output of the device without Alq_3. Quasisinusoidal variation of current efficiency versus Alq_3 thickness is attributed to the interference effect between direct emission and emission reflected from the metallic mirrors of the electrodes. This behavior has already been reported.[13,17] However, the effect of light out coupling *enhancement* due to the BEF film is increased and shows a strong dependendence on the device structure itself. This enhancement is calculated and the results are shown in Table I, where the values of k (given by $k = I_{\text{film}}/I_{\text{air}}$) are listed.

Pictiva EX2014
Samsung v Pictiva
IPR2024-00855

TABLE I. Factor of absolute light out coupling enhancement k and ratio between the output of the surface modified devices and the light intensity, which is coupled into the substrate (I_{film}/I_{gel}).

Alq_3-layer thickness (nm)	$k=I_{film}/I_{air}$	I_{film}/I_{gel}
0	1.30	0.63
10	1.27	0.60
30	1.80	0.63
50	2.04	0.60
70	2.25	0.58

Using a substrate surface modification, a fraction of the waveguided light retained within the substrate of the unmodified device (standard flat glass substrate) is extracted. In order to investigate the dependence of k on the device structure, the intensity I_{gel}, which is related to the sum of the external light output and the substrate waveguided light, was measured for all (unmodiefied) devices as a function of the Alq_3 layer thickness. Figure 4 shows the measured intensities I_{air} and I_{gel}. With increasing Alq_3 layer thickness the intensity I_{gel} decreases to 2/3 of the value for the device without Alq_3.

Table II shows the ratio between the amount of substrate waveguided light to the external light output for each device structure used in this study. This ratio is given by $I_{subst}/I_{air} = (I_{gel}-I_{air})/I_{air}$. With increasing Alq_3 layer thickness, the fraction of substrate waveguided light intensity increases compared to the fraction of the out coupled light intensity. This was further studied by means of the optical simulation tool.

In the simulation, the ratio I_{air}/I_{gel} based on the measurements was fitted by the ratio between the simulated amount of light, which is generated in the device stack and the simulated amount of light coupled into the substrate (Fig. 5). This ratio obtained by the simulation is given by the calculation of the power radiated outside of the cavity for air ($n_a=1$) as an outside medium with respect to glass ($n_a=1.52$) as an outside medium. In order to compute the ratio based on simulation,

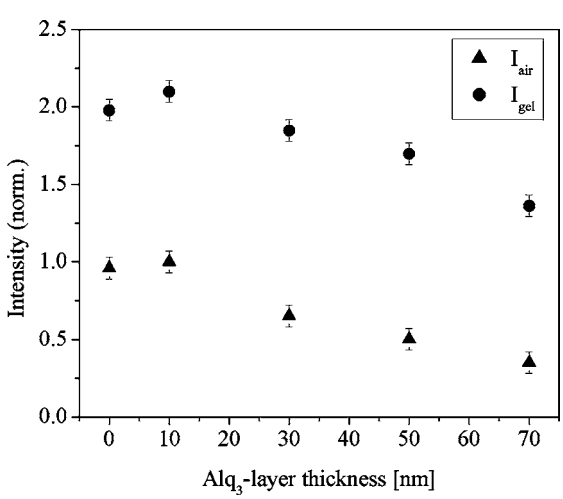

FIG. 4. The emission intensities detected by the Si photodiode at the air and gel gaps before substrate surface modification of the devices. The intensities are normalized on the output of the light output of the device with a Alq_3-layer thickness of 10 nm. The error bars represent the standard deviations of the measured values.

TABLE II. Calculated amount of waveguided light I_{subst} and ratio $I_{subst}:I_{air}$.

Alq_3-layer thickness (nm)	I_{air}	I_{gel}	$I_{subst}=I_{gel}-I_{air}$	Ratio $I_{subst}:I_{air}$
0	0.96	1.98	1.02	1.06
10	1.00	2.10	1.10	1.10
30	0.65	1.85	1.20	1.85
50	0.50	1.70	1.20	2.4
70	0.35	1.36	1.01	2.88

the location of the emission zone (EMZ) in the device is needed. Here, we have defined the location of the EMZ as the distance between the cathode and the center of a Gaussian distribution of excitons within the light emitting polymer with a full width at half maximum of 20 nm.[18] The distance between the EMZ and the cathode was varied to obtain the best fit. The resultant dependence of the location of the EMZ is shown in Fig. 5. Also shown is the location of the EMZ obtained by the fit. Except for the prediction of the model for 70 nm thickness of Alq_3, it is seen that the location of the EMZ scales with the actual device architecture.

The simulation as implemented above used the ratio I_{air}/I_{gel}, which does not depend on the actual light outcoupled at the glass-air interface for each device. With the location of the EMZ obtained by the fit, we can now see the effect of device architecture on the extent to which light is outcoupled depending on the cavity as defined by the OLED stack and substrate. Accordingly Fig. 6 shows the measurements of the external light output and the computed light output as a function of Alq_3 layer thickness at a fixed current density. It is observed that the light output calculated here (red symbols) decreases steadily with increasing Alq_3 layer thickness. However, it is important to note that the experimentally measured light output (black symbols) shows a more exaggerated dependence on Alq_3 thickness. This is due to variation in the internal device quantum efficiency as a function of Alq_3 thickness. In spite of this, the fit of I_{air}/I_{gel} is more accurate. This is because the ratio I_{air}/I_{gel} automatically eliminates the dependence on internal device efficiency.

Figure 7 shows the EL pattern (the power per unit solid

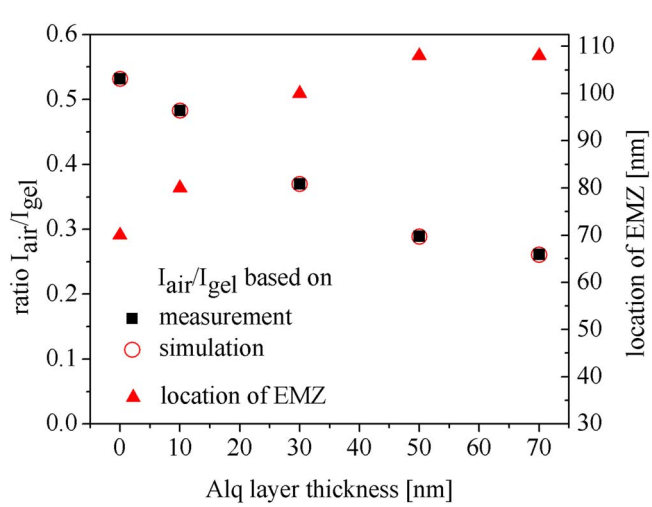

FIG. 5. (Color online) Fit of the ratio I_{gel}/I_{air} based on the shown dependence of the location of the EMZ.

Pictiva EX2014
Samsung v Pictiva
IPR2024-00855

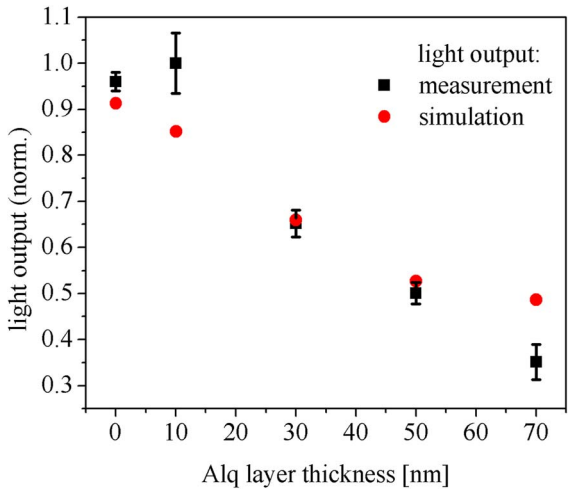

FIG. 6. (Color online) Measurements of the external light output and computed light output as a function of Alq_3-layer thickness. The effect of different Alq_3-layer thicknesses on the intrinsic device efficiency is not considered for the simulated values.

angle radiated outside the microcavity) integrated over all wavelengths for different Alq_3 thicknesses, which was obtained by simulation using the values for the location of the EMZ determined by the fit. The angle of 0° corresponds to the direction normal to the substrate, where the angle of 90° corresponds to the direction parallel to the substrate. With increasing values of Alq_3 layer thickness the distribution of intensity is shifted to higher angles with respect to the normal of the substrate (0°). As the intensity distribution shifts to higher angles, there will be an increase in light losses within the substrate due to TIR.

We can now consider the efficiency of light outcoupling by usual substrate surface modification techniques as a function of device architecture.

In the case of unmodified devices, with increasing Alq_3 layer thickness, the fraction of substrate waveguided light compared to the fraction of the external light output increases (Table I) as a result of the shift of the EL pattern to higher angles (see Fig. 7). Only the photons, which are emitted by the EML in a lower angle, defined by the escape cone of the substrate are extracted out of the device. After applying the BEF film, photons of higher emission angles can be extracted due to the prismatic structure of the film. The higher the fraction of substrate waveguided light, the stronger is the light outcoupling enhancement of the BEF film.

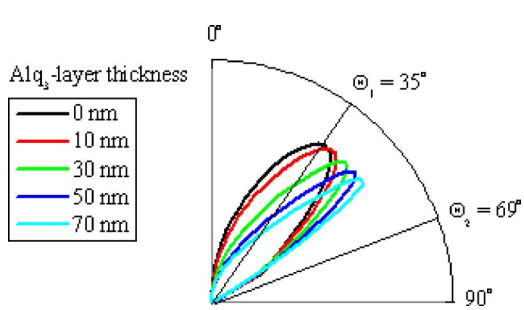

FIG. 7. (Color online) Normalized EL pattern of the devices used in this study (integrated over all wavelengths). Θ_1 and Θ_2 are the critical angles for substrate wave guiding respective anode/organic waveguiding.

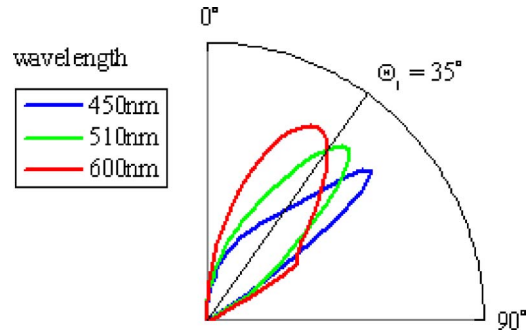

FIG. 8. (Color online) EL pattern of the device without Alq_3 layer for the wavelengths of 450, 510, and 600 nm. Each distribution is normalized on its intensity maximum.

Thus, the light outcoupling enhancement obtained by calculating the ratio between the light output of the surface modified and the output of the unmodified device by itself does not lead to accurate conclusions about the efffictiveness of the light outcoupling method. Instead, the performance of the BEF film can be determined by considering the ratio between the external output of the BEF film laminated device and the total amount of light, which is measured with the gel. This ratio is given by I_{film}/I_{gel} and is approximately constant ($I_{film}/I_{gel} \approx 0.6$, Table I) for all device structures. By the means of the BEF film about 60% of the light, which is coupled into the substrate, is extracted out of each modified device.

In all of the above calculations, the cavity effect was simulated over the entire range of wavelengths comprising the device spectrum. We furthermore discuss the dependence of the light outcoupling enhancement factor k (apparent light outcoupling enhancement) on the wavelength of the emitted light. In this case we consider the device without the Alq_3 layer. Figure 8 shows the EL pattern for light of wavelengths of 450, 510, and 600 nm calculated using the microcavity simulation mentioned above. 510 nm is the peak wavelength of the used green emitter. The calculations for the wavelengths of 450 and 600 nm were computed, in order to obtain typical distributions for blue and red emissions, respectively. The EL pattern for 450 nm is shifted to higher angles in comparison to that obtained for 510 nm. Thus, we hypothesize that the fraction of waveguided light is higher for the blue emitting device than for the green emitting device. Hence, the light outcoupling enhancement due to substrate surface modification is higher for the blue emitting device than for the green emitting device. Contemplating the imaginary red emitting device, the EL pattern of the red emitting device is shifted to lower angles. In this case, we hypothesize that the fraction of waveguided light is lower than for the green emitting device. This leads to a lower light outcoupling enhancement for the red device due to the same substrate surface modification technique.

In particular, the dependence of light outcoupling enhancement on the wavelength has to be considered when modifying the substrate surface of a device emitting in a broad range of wavelengths (for example, a white light emitting device). In the case of a device with the structure and location of the EMZ discussed above, the light outcoupling

Pictiva EX2014
Samsung v Pictiva
IPR2024-00855

enhancement is expected to be stronger in the shorter wavelength range of the spectrum. Thus, substrate surface modification can result in differences between the spectrum of the device before and after surface modification for light extraction.

IV. CONCLUSION

In conclusion we have demonstrated that the apparent effectiveness of light outcoupling enhancement using a method of modifying the substrate surface is significantly dependent on the device structure itself. This apparent effectiveness, however, is not the correct value to judge the effectiveness of a technique to enhance light out coupling due to substrate surface modification. The ratio between the light output of the surface modified device and the total amount of light which is generated in the device stack and coupled into the substrate (before the substrate/air interface) is a more accurate parameter to describe the light enhancement properties. In the optimal case the ratio is 1, which corresponds to a light outcoupling methodology completely suppressing substrate waveguiding. Determination of the enhancement properties using the proposed method not only allows the comparison of different methods of substrate surface modifying techniques but also provides an analytical understanding to enable further improvement of each technique.

Furthermore, we have shown a wavelength dependence of the apparent effectiveness of light outcoupling enhancement due to substrate surface modification. This is another reason why the apparent effectiveness is not the correct value to judge the effectiveness of a substrate surface modification. The dependence of the apparent light outcoupling enhancement leads to changes in the output spectrum, when modifying the substrate surface of an organic electroluminescences (EL) device emitting in a broad range of wavelengths.

ACKNOWLEDGMENTS

We would like to thank Dr. Ralph Pätzold and Dirk Buchhauser for useful discussions. This work is supported by the Department of Energy (Polymer OLED White Light Development Program Award No. DE-FC26-04NT41947).

[1] S. Moeller and S. R. Forrest, J. Appl. Phys. **91**, 3324 (2002).
[2] V. Bulovic, V. B. Khalfin, G. Gu, P. E. Burrows, D. Z. Garbuzov, and S. R. Forrest, Phys. Rev. B **58**, 3730 (1998).
[3] A. R. Duggal, J. J. Shiang, C. M. Heller, and D. F. Foust, Appl. Phys. Lett. **80**, 3470 (2002).
[4] M. Scheffel, A. Hunze, J. Birnstock, J. Blässing, W. Rogler, G. Wittmann, and A. Winnacker, *Enhanced Light Extraction by Substrate Modification of Organic Electroluminescent Devices*, Proceedings of the European Conference on Organic Electronics and Related Phenomena '01, p. 158 (2001).
[5] M.-H. Lu, C. F. Madigan, and J. C. Sturm, Tech. Dig. - Int. Electron Devices Meet. **2000**, 607.
[6] G. Gu, D. Z. Garbuzov, P. E. Burrows, S. Venkatesh, S. R. Forrest, and M. E. Thomson, Opt. Lett. **22**, 396 (1997).
[7] T. Tsutsui, M. Yahiro, H. Yokogawa, K. Kawano, and M. Yokoyama, Adv. Mater. (Weinheim, Ger.) **13**, 1149 (2001).
[8] R. H. Jordan, L. J. Rothberg, A. Dodabalapur, and R. E. Slusher, Appl. Phys. Lett. **69**, 1997 (1996).
[9] H. J. Peng, M. Wong, and H. S. Kwok, SID Int. Symp. Digest Tech. Papers **34**, 516 (2003).
[10] J. M. Lupton, B. J. Matterson, I. D. W. Samuel, M. J. Jory, and W. L. Barnes, Appl. Phys. Lett. **77**, 3340 (2000).
[11] M. G. Salt, W. L. Barnes, and I. D. W. Samuel, J. Mod. Opt. **48**, 1085 (2001).
[12] X. H. Yang and D. Neher, Appl. Phys. Lett. **84**, 2476 (2004).
[13] T. Nakamura, N. Tsutsumi, N. Juni, and H. Fujii, J. Appl. Phys. **96**, 6016 (2004).
[14] www.unicadinc. com
[15] J.-S. Kim, P. K. H. Ho, N. C. Greenham, and R. H. Friend, J. Appl. Phys. **88**, 1073 (2000).
[16] V. Bulovic, V. B. Khalfin, G. Gu, P. E. Burrows, D. Z. Garbuzov, and S. R. Forrest, Phys. Rev. B **58**, 3730 (1998).
[17] M. Matsumura and T. Furukawa, Jpn. J. Appl. Phys., Part 1 **41**, 2742 (2002).
[18] Z. Wu, L. Wang, G. Lei, and Y. Qiu, J. Appl. Phys. **97**, 103105 (2005).

Pictiva EX2014
Samsung v Pictiva
IPR2024-00855